Suppression of lethal autoimmunity by regulatory T cells with a single TCR specificity

Andrew G. Levine,[1] Saskia Hemmers,[1] Antonio P. Baptista,[2] Michail Schizas,[1] Mehlika B. Faire,[1] Bruno Moltedo,[1] Catherine Konopacki,[1] Marc Schmidt-Supprian,[3] Ronald N. Germain,[2] Piper M. Treuting,[4] and Alexander Y. Rudensky[1]

[1]Howard Hughes Medical Institute, Immunology Program, Ludwig Center, Memorial Sloan-Kettering Cancer Center, New York, NY 10065
[2]Lymphocyte Biology Section, Laboratory of Systems Biology, National Institute of Allergy and Infectious Diseases, National Institutes of Health, Bethesda, MD 20892
[3]Hematology and Oncology, Klinikum rechts der Isar, Technische Universität München, 80333 Munich, Germany
[4]Department of Comparative Medicine, University of Washington School of Medicine, Seattle, WA 98195

The regulatory T cell (T reg cell) T cell receptor (TCR) repertoire is highly diverse and skewed toward recognition of self-antigens. TCR expression by T reg cells is continuously required for maintenance of immune tolerance and for a major part of their characteristic gene expression signature; however, it remains unknown to what degree diverse TCR-mediated interactions with cognate self-antigens are required for these processes. In this study, by experimentally switching the T reg cell TCR repertoire to a single T reg cell TCR, we demonstrate that T reg cell function and gene expression can be partially uncoupled from TCR diversity. An induced switch of the T reg cell TCR repertoire to a random repertoire also preserved, albeit to a limited degree, the ability to suppress lymphadenopathy and T helper cell type 2 activation. At the same time, these perturbations of the T reg cell TCR repertoire led to marked immune cell activation, tissue inflammation, and an ultimately severe autoimmunity, indicating the importance of diversity and specificity for optimal T reg cell function.

INTRODUCTION

Increased thymic generation of regulatory T cells (T reg cells) resulting from coexpression of transgene-encoded TCRs and their cognate ligands provided early experimental evidence that T reg cell differentiation is dependent on self-antigen recognition in the thymus (Jordan et al., 2001). Transgene-driven expression of naturally occurring T reg cell–derived TCRs, however, has been found to yield few T reg cells, with the majority of transgenic TCR-expressing cells differentiating into conventional CD4 T cells (Bautista et al., 2009; Leung et al., 2009). This feature of T reg cell differentiation, ascribed to a profound intraclonal competition among thymic T reg cell precursors, implies a stringent requirement for TCR diversity during T reg cell differentiation. Antigen presentation in the periphery is thought to mirror the thymus (Anderson et al., 2002), and analogously, limiting amounts of tissue-specific self-antigens presented in draining lymph nodes likely maintain the activation status of small numbers of antigen-specific T reg cells (Samy et al., 2005; Leventhal et al., 2016). Nevertheless, it remains unknown whether diverse T reg cell specificities molded through recognition of a wide range of endogenous antigens during thymic differentiation and peripheral maintenance are required for restraining a broad spectrum of autoimmune and inflammatory lesions that T reg cells normally control.

Recently, we and others demonstrated that the T reg cell TCR controls expression of a large number of genes in activated T reg cells and is required for suppressor function such that TCR loss in Foxp3-expressing T reg cells results in spontaneous immune activation and an early onset, highly aggressive fatal lymphoproliferative disease comparable with that observed in Foxp3-deficient mice lacking T reg cells (Levine et al., 2014; Vahl et al., 2014). However, these previous studies left open a question of which TCR-dependent gene expression features might be exhibited by T reg cells expressing just a few or even a single TCR specificity and whether these cells might afford any measure of protection against systemic disease and tissue pathology.

In this regard, we recently reported that loss of TCRs within a lower-affinity range for self-ligands in the developing T reg cell population in the absence of the intronic *Foxp3* enhancer CNS3 had a mild effect on immune activation status without detectable clinical manifestations of autoimmunity, suggesting that a reduced T reg cell repertoire with holes was largely sufficient to support the bulk of T reg cell suppressor function (Feng et al., 2015). However, the severe autoimmunity apparent in mice with a combined deficiency in CNS3 and the autoimmune regulator (*Aire*) gene, which among other functions facilitates elimination of tissue-

Correspondence to Alexander Y. Rudensky: rudenska@mskcc.org

Abbreviations used: DT, diphtheria toxin; eGFP, enhanced GFP; RAG, recombination-activating gene.

The Rockefeller University Press $30.00
J. Exp. Med. 2017 Vol. 214 No. 3 609–622
https://doi.org/10.1084/jem.20161318

restricted antigen-specific effector T cells and differentiation of T reg cells of corresponding specificities in the thymus, suggests an important role for T reg cell TCR specificities in establishing tolerance early in life (Samy et al., 2005; Feng et al., 2015; Yang et al., 2015; Malchow et al., 2016).

Efforts to directly address the role of TCR diversity and specificity for T reg cell function through the use of TCR transgenic mice have been impeded by an inevitable concomitant severe skewing of the effector CD4 T cell repertoire. Thus, although in recombination-activating gene (RAG)–deficient TCR transgenic mice antigen-specific T reg cells can keep in check effector T cells of the same specificity and prevent pathology (Killebrew et al., 2011; Lin et al., 2016), it is unknown whether a monoclonal T reg cell population can suppress a naturally diverse effector T cell pool. Here, we addressed this question by exploring whether lethal autoimmunity exerted by a diverse effector T cell population upon the loss of T reg cell function can be restrained by T reg cells subjected to inducible skewing of their developmentally selected TCR repertoire to a single endogenous T reg cell–derived TCR. Unexpectedly, in the presence of T reg cells expressing a single TCR, we observed lasting, even if incomplete, protection from lethal disease resulting from complete ablation of the TCR in T reg cells, with diminished T cell activation and T helper cell type 2 (Th2 cell) and Th17 cytokine production in select secondary lymphoid organs. Moreover, expression of this single TCR also rescued the majority of the gene signature imparted by a diverse T reg cell TCR repertoire. Finally, we also observed limited but measurable immunosuppressive function in T reg cells subjected to inducible replacement of their endogenous repertoire with TCR specificities that are not subject to ligand-based thymic selection. These results indicate that T reg cells can mediate substantial control of autoimmune reactivity even with a monoclonal or altered TCR repertoire, although optimal immune homeostasis may demand a more diverse recognition capacity for self-antigens.

RESULTS AND DISCUSSION

Monoclonal G113 TCR$^+$ T reg cells suppress a diverse effector T cell pool

To directly assess the role of T reg cell TCR diversity in driving suppressor function, we took advantage of the previously characterized T reg cell–derived V$\beta6^+$V$\alpha2^+$ G113 TCR. The G113 TCR, originally cloned out of the CD4$^+$CD25$^+$ cell pool in TCli TCRβ-expressing *Tcra*$^{+/-}$ mice, is a T reg cell TCR that induces strong signaling as well as proliferation and expansion when expressed in T cells in in-vivo transfer experiments but, when expressed as a transgene on a RAG-deficient background, generates a preponderance of conventional CD4 T cells and few Foxp3$^+$ thymocytes (Hsieh et al., 2004, 2006; Moran et al., 2011). This effect has been observed for the majority of T reg cell TCRs characterized so far (Bautista et al., 2009; Leung et al., 2009). Expression of the G113Tg on a RAG-sufficient background results in highly efficient allelic exclusion of the endogenous *Tcrb* locus such that ∼95% of T reg cells in G113Tg mice exclusively express the transgenic V$\beta6^+$ TCRβ chain (Fig. 1 A). Accordingly, as compared with T reg cells in non–G113Tg-expressing mice, Foxp3$^+$ cells in G113Tg mice demonstrated minimal staining for endogenous Vβ5, Vβ8.1/2, Vβ11, Vβ12, and Vβ13 TCRβ chains (Fig. 1 B). In contrast, less than half of T reg cells expressed the V$\alpha2^+$ TCRα transgene (see Fig. 2 A). As a result, the majority of T reg cells in these mice were selected by TCRs composed of the transgenic V$\beta6^+$ TCRβ chain paired with an endogenous TCRα chain. To enable replacement of diverse TCRs resulting from endogenous *Tcra* locus rearrangements with predominantly the single transgenic G113 TCR after Foxp3 induction, i.e., T reg cell lineage commitment, we generated G113Tg*Foxp3*$^{YFP\text{-}Cre}$*Tcra*$^{FL/FL}$ mice on a RAG-sufficient background (Fig. 1, A–C). In these mice, Foxp3 expression in developing T reg cells resulted in Cre recombinase–mediated ablation of the endogenous *Tcra* locus, leaving only the G113 V$\alpha2^+$ TCRα chain to pair with transgenic TCRβ (Fig. 1, A–C). Thus, in G113Tg*Foxp3*$^{YFP\text{-}Cre}$*Tcra*$^{FL/FL}$ mice, T reg cells were thymically generated in physiological numbers via expression of endogenous TCRs that recognize endogenous ligands, whereas the peripheral T reg cell compartment was overwhelmingly of a single, monoclonal specificity. Unique to this experimental set-up was the retention of significant diversity in the effector T cell population, with the majority of effector CD4$^+$ T cells expressing endogenously rearranged TCRα chains (Fig. 1 C).

As we previously reported, all *Foxp3*$^{YFP\text{-}Cre}$*Tcra*$^{FL/FL}$ mice suffered from an early onset lethal autoimmunity characterized by runting and scaly skin and did not survive past 4 wk of age (Fig. 1, D and E; Levine et al., 2014). Unexpectedly, G113Tg*Foxp3*$^{YFP\text{-}Cre}$*Tcra*$^{FL/FL}$ mice were visibly indistinguishable from control mice bearing normal populations of T reg cells during the first weeks of life (Fig. 1 D). Although by 6 wk of age, some G113Tg*Foxp3*$^{YFP\text{-}Cre}$*Tcra*$^{FL/FL}$ mice began to show signs of decreased weight gain and variable skin disease and ultimately succumbed to disease, several mice continued to show minimal outward signs of autoimmunity. A striking 50% of mice survived to 4 mo of age, the end point of the experiment, at which point all mice displayed visible evidence of significant autoimmunity (Fig. 1 E and not depicted).

Consistent with immune activation observed in G113Tg*Foxp3*$^{YFP\text{-}Cre}$*Tcra*$^{FL/FL}$ mice even at an early age despite increased survival in comparison with *Foxp3*$^{YFP\text{-}Cre}$*Tcra*$^{FL/FL}$ mice, analysis of histopathology in 2.5-wk-old mice demonstrated widespread tissue inflammation in G113Tg*Foxp3*$^{YFP\text{-}Cre}$*Tcra*$^{FL/FL}$ compared with control *Foxp3*$^{YFP\text{-}Cre}$*Tcra*$^{WT/FL}$ and G113Tg*Foxp3*$^{YFP\text{-}Cre}$*Tcra*$^{WT/FL}$ mice (Fig. 1, F and G). However, pathology was notably diminished in G113Tg*Foxp3*$^{YFP\text{-}Cre}$*Tcra*$^{FL/FL}$ compared with *Foxp3*$^{YFP\text{-}Cre}$*Tcra*$^{FL/FL}$ mice; critically, this effect did not appear to be the consequence of limited autoreactivity caused by G113Tg expression on the effector T cell compartment, as G113Tg*Foxp3*^{KO} mice suffered from lethal autoimmunity largely indistinguishable from that of *Foxp3*^{KO} mice lacking the TCR transgene (Fig. 1, D and

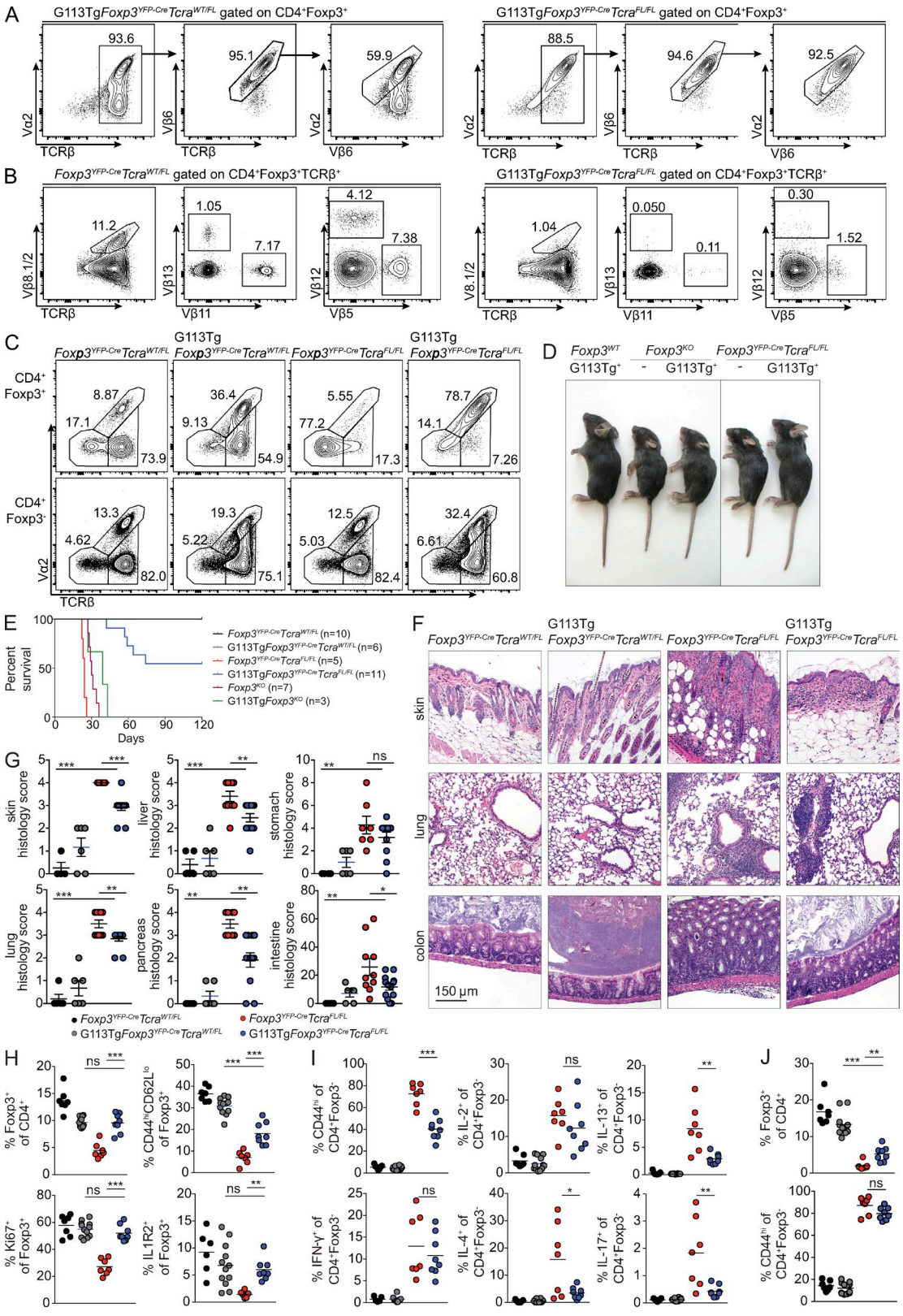

Figure 1. **Monoclonal G113 TCR-expressing T reg cells suppress autoimmune disease mediated by a polyclonal effector T cell population.** (A–J) Mice of the indicated genotypes were analyzed at 2.5 wk of age. (A and B) Representative flow cytometry plots of TCR Vα and Vβ usage in $CD4^+Foxp3^+$ (A) and $CD4^+Foxp3^+TCR\beta^+$ (B) lymph node cells in the indicated mice. Further gating of the indicated cellular subsets is indicated by arrows. (C) Representative

E; and not depicted; Fontenot et al., 2003). This result suggests that rescue of disease in G113Tg*Foxp3*$^{YFP\text{-}Cre}$*Tcra*$^{FL/FL}$ mice was caused by the effects of transgenic TCR expression specifically in the T reg cell compartment.

Indeed, the G113Tg in G113Tg*Foxp3*$^{YFP\text{-}Cre}$*Tcra*$^{FL/FL}$ mice fully rescued percentages and proliferation (as assessed by Ki67 staining) of lymph node T reg cells, significantly rescued effector differentiation as assessed by CD44 and CD62L expression, and restored cell-surface expression of the receptor IL-1R2, among others, on T reg cells (Fig. 1 H). Lymph node effector CD4 T cell activation was correspondingly diminished, with decreased percentages of CD44^{hi} and IL-4–, IL-13–, and IL-17– but not IFNγ- or IL-2–producing cells (Fig. 1 I). However, in the spleen, where rescue of T reg cell percentages was modest, effector T cell activation was not lessened (Fig. 1 J and not depicted). T cell activation and cytokine production were similar between *Foxp3*^{KO} and G113Tg*Foxp3*^{KO} mice in both spleens and lymph nodes, further ruling out a major intrinsic role for the G113Tg in decreasing effector T cell activation (not depicted). Thus, the degree of G113Tg-mediated T reg cell rescue correlated with the degree of suppression of effector T cell activation. This further supported an essential role of monoclonal G113 TCR-expressing T reg cells in down-modulating autoimmunity, although only to a limited degree, in G113Tg*Foxp3*$^{YFP\text{-}Cre}$*Tcra*$^{FL/FL}$ mice.

Inducible replacement of the diverse TCR repertoire with the G113 TCR in mature T reg cells

Given that T reg cells undergo TCR-dependent maturation in the periphery, we sought to test whether mature T reg cells, which had seeded the spleen and tissues and were then subjected to inducible replacement of their TCRs with the G113 TCR, remained functionally competent or were impaired in their ability to control immune activation, like T reg cells in *Foxp3*$^{eGFP\text{-}CreERT2}$*Tcra*$^{FL/FL}$ mice (Levine et al., 2014). Therefore, we generated G113Tg*Foxp3*^{CreERT2}*Tcra*$^{FL/FL}$ mice to enable the switch of endogenous T reg cell TCRs in mature T reg cells in adult mice for the G113 TCR in a tamoxifen-inducible manner (Fig. 2 A). 2 wk of tamoxifen administration to G113Tg*Foxp3*^{CreERT2}*Tcra*$^{FL/FL}$ mice resulted in clear increases in immune activation compared with control G113Tg*Foxp3*^{CreERT2}*Tcra*$^{WT/WT}$ mice (Fig. 2, B–D). This result indicates that the G113 TCR was not sufficient to impart full TCR-dependent T reg cell function in the periphery, even in a normally differentiated and localized T reg cell population.

We turned to an in vivo adoptive transfer approach to enable a more stringent assessment for suppressor activity of T reg cells whose diverse TCRs had been inducibly switched to the G113 TCR in comparison with T reg cells expressing diverse TCRs and T reg cells subjected to TCR ablation. We FACS sorted bulk T reg cells from *Foxp3*^{CreERT2}*Tcra*$^{WT/WT}$ mice, Vβ6$^+$ T reg cells from G113Tg*Foxp3*^{CreERT2}*Tcra*$^{WT/WT}$ mice, G113$^+$ (Vβ6$^+$Vα2$^+$) T reg cells from G113Tg-*Foxp3*^{CreERT2}*Tcra*$^{FL/FL}$ mice, and TCR-deficient (TCRβ$^-$) T reg cells from *Foxp3*^{CreERT2}*Tcra*$^{FL/FL}$ mice. All groups of mice in these experiments were subjected to identical tamoxifen treatment (two doses on days −7 and −6 before sorting on day 0; Fig. 2 E). Sorted cells were transferred together with fully polyclonal preactivated effector CD4 T cells isolated from T reg cell–depleted CD45.1$^+$*Foxp3*^{DTR} mice into T cell–deficient *Tcrb*$^{-/-}$*Tcrd*$^{-/-}$ recipients that were analyzed 4 wk after transfer (Fig. 2 E). In agreement with the markedly diminished disease observed in G113Tg*Foxp3*$^{YFP\text{-}Cre}$*Tcra*$^{FL/FL}$ mice, cotransfer of G113$^+$ T reg cells but not of TCR-deficient T reg cells substantially decreased parameters of immune activation including lymphadenopathy, CD4 T cell numbers, and IFN-γ production in lymph nodes but not in spleens of recipient mice (Fig. 2 F). These results confirm the capacity of monoclonal G113$^+$ T reg cells to exert significant but incomplete suppressor activity, in comparison with a T reg cell population expressing a diverse TCR repertoire. These observations raised a question of whether the inability of T reg cells expressing a single TCR to fully control immune activation was because of its inability to impart a complete range of TCR-dependent gene expression or rather was because of limiting TCR ligand–driven activation restricted to specific local settings.

Rescue of the T reg cell TCR-dependent gene signature by monoclonal G113 TCR expression

Previously, we used microarray gene expression analysis to identify a set of TCR-dependent genes expressed in CD44^{hi}CD62L^{lo} effector and CD44^{lo}CD62L^{hi} naive T reg cells (Levine et al., 2014). In that study, analysis of TCR-sufficient and -deficient T reg cells showed that TCR-dependent gene expression accounted for ∼25% of the gene signature

flow cytometric analysis of lymph node CD4$^+$Foxp3$^+$ (top) and CD4$^+$Foxp3$^-$ (bottom) cells in mice of the indicated genotypes. (D) Representative mice of the indicated genotypes. (E) Survival curve for the indicated mice. (F) Representative hematoxylin and eosin staining of tissue sections from mice of the indicated genotypes. (G) Histology scores of tissues from *Foxp3*$^{YFP\text{-}Cre}$*Tcra*$^{WT/FL}$ (black circles), G113Tg*Foxp3*$^{YFP\text{-}Cre}$*Tcra*$^{WT/FL}$ (gray circles), *Foxp3*$^{YFP\text{-}Cre}$*Tcra*$^{FL/FL}$ (red circles), and G113Tg*Foxp3*$^{YFP\text{-}Cre}$*Tcra*$^{FL/FL}$ (blue circles) mice. (H) Percent Foxp3$^+$ cells among CD4$^+$ cells (top left) and percent Ki-67$^+$ (bottom left), percent CD44^{hi}CD62L^{lo} (top right), and IL-1R2$^+$ (bottom right) cells among Foxp3$^+$ cells in the lymph nodes of mice of the indicated genotypes (as in G). (I) CD4^{+-} Foxp3$^-$ T cell activation and cytokine production in lymph nodes of the indicated mice. (J) The percent Foxp3$^+$ of CD4$^+$ T cells (top) and percent CD44^{hi} of CD4$^+$Foxp3$^-$ cells (bottom) in spleens of the indicated mice. Each circle represents an individual mouse. The horizontal bars represent mean value. P-values were calculated using unpaired Student's *t* test. *, $P < 0.05$; **, $P < 0.01$; ***, $P < 0.001$. Flow cytometry plots and hematoxylin and eosin sections are representative of at least three independent experiments with at least two mice of each genotype per experiment. Graphs show the combined results of at least five independent experiments with at least one mouse per genotype per experiment.

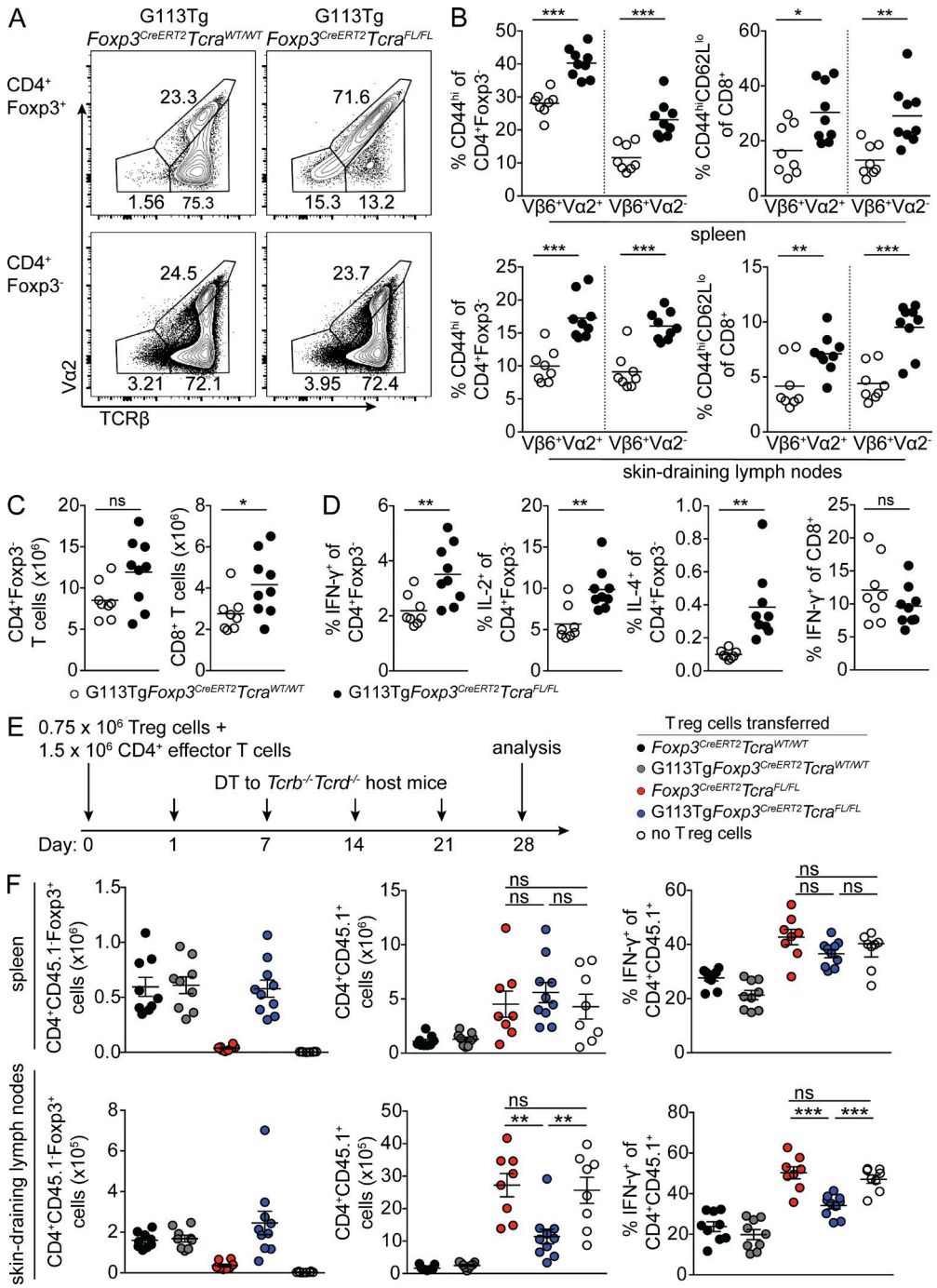

Figure 2. **Inducible replacement of the diverse TCR repertoire with the G113 TCR in mature T reg cells.** (A–D) G113Tg*Foxp3*^{CreERT2}*Tcra*$^{WT/WT}$ and G113Tg*Foxp3*^{CreERT2}*Tcra*$^{FL/FL}$ mice were treated with tamoxifen on days 0, 3, 7, and 10 and analyzed on day 13. (A) Representative flow cytometric analyses of lymph node CD4$^+$Foxp3$^+$ (top) and CD4$^+$Foxp3$^-$ (bottom) cells in G113Tg*Foxp3*^{CreERT2}*Tcra*$^{WT/WT}$ (left) and G113Tg*Foxp3*^{CreERT2}*Tcra*$^{FL/FL}$ (right) mice. (B) CD4^{+-} Foxp3$^-$ (left) and CD8$^+$ (right) T cell activation in spleens (top) and lymph nodes (bottom) of G113Tg*Foxp3*^{CreERT2}*Tcra*$^{WT/WT}$ (open circles) and G113Tg*Foxp3*^{CreERT2} *Tcrac*$^{FL/FL}$ (closed circles) mice. CD4$^+$Foxp3$^-$ and CD8$^+$ cells were further gated as either Vβ6$^+$Vα2$^+$ (G113$^+$) or Vβ6$^+$Vα2$^-$ (G113$^-$) cells. (C and D) T cell numbers in lymph nodes (C) and cytokine production in spleens (D) of mice of the indicated genotypes, as in B. (E and F) In vivo suppression assay. (E) Schematic of the experiment. T reg cells were sorted from the following mice on day 0 after tamoxifen administration on days −7 and −6: bulk T reg cells from *Foxp3*^{CreERT2} *Tcra*$^{WT/WT}$ mice (black circles), Vβ6$^+$ T reg cells from G113Tg*Foxp3*^{CreERT2}*Tcra*$^{WT/WT}$ mice (gray circles), TCRβ$^-$ T reg cells from *Foxp3*^{CreERT2}*Tcra*$^{FL/FL}$ mice (red circles), and Vβ6$^+$Vα2$^+$ T reg cells from G113Tg*Foxp3*^{CreERT2}*Tcra*$^{FL/FL}$ mice (blue circles). CD4 effector T cells were isolated on day 0 from CD45.1$^+$*Foxp3*^{DTR} mice treated with DT on days −5, −4, and −1. On day 0, T reg cells and effector CD4 T cells were transferred into *Tcrb*$^{-/-}$*Tcrd*$^{-/-}$ mice subsequently maintained on weekly doses of DT until analysis on day 28. (F) Numbers of CD45.2$^-$CD4$^+$Foxp3$^+$ T reg cells (left) and CD45.1$^+$CD4$^+$Foxp3$^-$ cells (middle) and percent IFN-γ$^+$

specific to activated T reg cells. To address the major question of whether a single TCR specificity can enable a full or only partial spectrum of T reg cell gene expression, we performed RNA sequencing (RNA-seq) analysis on effector and naive TCR^+ and TCR^- T reg cells from *Foxp3*^{CreERT2}*Tcra*$^{FL/WT}$ mice as well as effector and naive TCR^+ and TCR^- T reg cells from immune-activated *Foxp3*^{CreERT2}*Tcra*$^{FL/FL}$ mice. We also performed similar analysis for effector and naive T reg cells isolated from tamoxifen-treated G113Tg*Foxp3*^{CreERT2}*Tcra*$^{WT/WT}$ and G113Tg*Foxp3*^{CreERT2}*Tcra*$^{FL/FL}$ mice.

First, we isolated from RNA-seq data a complete set of TCR-dependent genes defined as all genes significantly up- or down-regulated in effector and naive TCR-sufficient compared with TCR-deficient T reg cells from healthy *Foxp3*^{CreERT2}*Tcra*$^{WT/FL}$ mice. To further extract a set of strictly TCR-dependent genes, we pared from this TCR-regulated gene set all genes whose expression in TCR-deficient T reg cells could be normalized by TCR-independent inputs resulting from the immune activation and inflammation observed in *Foxp3*^{CreERT2}*Tcra*$^{FL/FL}$ mice. For example, one such removed gene was *Ctla4*, whose expression was decreased in TCR-deficient compared with TCR-sufficient T reg cells in healthy *Foxp3*^{CreERT2}*Tcra*$^{WT/FL}$ mice but was fully rescued in TCR-deficient T reg cells in diseased *Foxp3*^{CreERT2}*Tcra*$^{FL/FL}$ mice. Our RNA-seq analysis identified 473 genes that were up- and 204 genes that were down-regulated in effector T reg cells in a strictly TCR-dependent manner and 143 genes that were up- and 38 genes that were down-regulated in naive T reg cells in a strictly TCR-dependent manner. Next, we determined the extent to which changes in expression of these genes induced upon TCR ablation in effector and naive T reg cells could be rescued upon expression of the G113 TCR transgene alone in G113Tg*Foxp3*^{CreERT2}*Tcra*$^{FL/FL}$ mice compared with G113 TCR transgene expression in combination with diverse endogenously rearranged TCRs in G113Tg-*Foxp3*^{CreERT2}*Tcra*$^{WT/WT}$ mice.

Strikingly, the monoclonal G113 T reg cell–derived TCR was able to support expression of the majority of genes whose expression was found to be TCR dependent in T reg cells expressing a diverse TCR repertoire (Fig. 3 A). Of the 473 genes we identified as up-regulated in a TCR-dependent manner in effector T reg cells, expression of 325 (69%) was fully rescued by expression of the monoclonal G113 TCR in G113Tg*Foxp3*^{CreERT2}*Tcra*$^{FL/FL}$ when compared with polyclonal T reg cells from G113Tg*Foxp3*^{CreERT2}*Tcra*$^{WT/WT}$ mice; these included genes coding for putative effectors and regulators of suppressor function *Tigit*, *Cxcl10*, *Il10*, *Lag3*, *Icos*, and *Pdcd1*; transcription factors *Irf4*, *Myb*, *Nfatc1*, *Nr4a3*, and *Relb*; and the chemokine receptor *Ccr8*. Although the strongly TCR-dependent genes *Egr2*, *Egr3*, *Il1r2*, *Ebi3*, and *Penk* were not fully rescued, the observed difference in their expression in polyclonal versus monoclonal T reg cells from G113Tg*Foxp3*^{CreERT2}*Tcra*$^{WT/WT}$ versus G113Tg*Foxp3*^{CreERT2} *Tcra*$^{FL/FL}$ mice was markedly less pronounced than that in TCR-sufficient versus -deficient T reg cells from *Foxp3*^{CreERT2} *Tcra*$^{FL/WT}$ mice. Similarly, of the 204 genes down-regulated in a TCR-dependent manner in effector T reg cells, 177 (87%) were fully rescued. A comparable, if not more profound, rescue of TCR-dependent gene expression was also observed for naive T reg cells. We found that 120 of 143 (84%) genes up-regulated in a TCR-dependent manner were similarly expressed or were actually overexpressed in naive monoclonal T reg cells in G113Tg*Foxp3*^{CreERT2}*Tcra*$^{FL/FL}$ mice compared with T reg cells in G113Tg*Foxp3*^{CreERT2}*Tcra*$^{WT/WT}$ mice expressing diverse endogenously rearranged TCRs. The latter set included the genes *Egr1*, *Egr2*, *Egr3*, *Cd5*, *Irf4*, *Myb*, and *Nab2*. Likewise, of the 38 genes down-regulated in naive T reg cells in a polyclonal TCR-dependent manner, 36 (95%) were fully rescued. Together, these data demonstrate that at a population level, G113 TCR expression rescues the vast majority, if not all, of the TCR-dependent transcriptional signature in both effector and naive T reg cell subsets.

Preferential activation of G113 TCR–expressing T reg cells in skin-draining lymph nodes

The demonstration of widespread rather than limited rescue of TCR-dependent gene expression in T reg cells by the monoclonal G113 TCR suggested that incomplete protection against autoimmune disease by these cells might be caused by activation limited to a particular local setting rather than because of limited TCR-dependent gene expression induced by a given single TCR. Thus, we next used flow cytometric analysis to examine expression of EGR2, as a representative TCR-dependent gene that was only partially rescued by the monoclonal G113 TCR in effector T reg cells (Fig. 3 A), hypothesizing that it could reveal site-specific signaling through the G113 TCR. In lymph node effector T reg cells, we observed that, compared with polyclonal T reg cells, a decreased portion of monoclonal $G113^+$ T reg cells were positive for EGR2 (69 ± 0.78% vs. 52 ± 5.7%), consistent with incomplete TCR-dependent activation of the monoclonal $G113^+$ effector T reg cell pool that might arise from limited ligand availability. TCR-deficient T reg cells used as a control showed negligible EGR2 expression (5 ± 0.2%). Conversely, consistent with RNA-seq data (Fig. 3 A), we noted that EGR2 was expressed at higher levels in naive monoclonal $G113^+$ T reg cells in the lymph nodes of G113Tg*Foxp3*^{CreERT2}*Tcra*$^{FL/FL}$ mice than in naive polyclonal T reg cells from G113Tg*Foxp3*^{CreERT2}

$CD45.1^+CD4^+$ cells (right) in spleens (top) and skin-draining lymph nodes (bottom). Each circle represents an individual mouse. The horizontal bars represent mean value. P-values were calculated using unpaired Student's *t* test. *, $P < 0.05$; **, $P < 0.01$; ***, $P < 0.001$. The data shown represent the combined results of three independent experiments with at least two mice per genotype each (A–D) or the combined results of two independent experiments with at least four mice per group each (E and F).

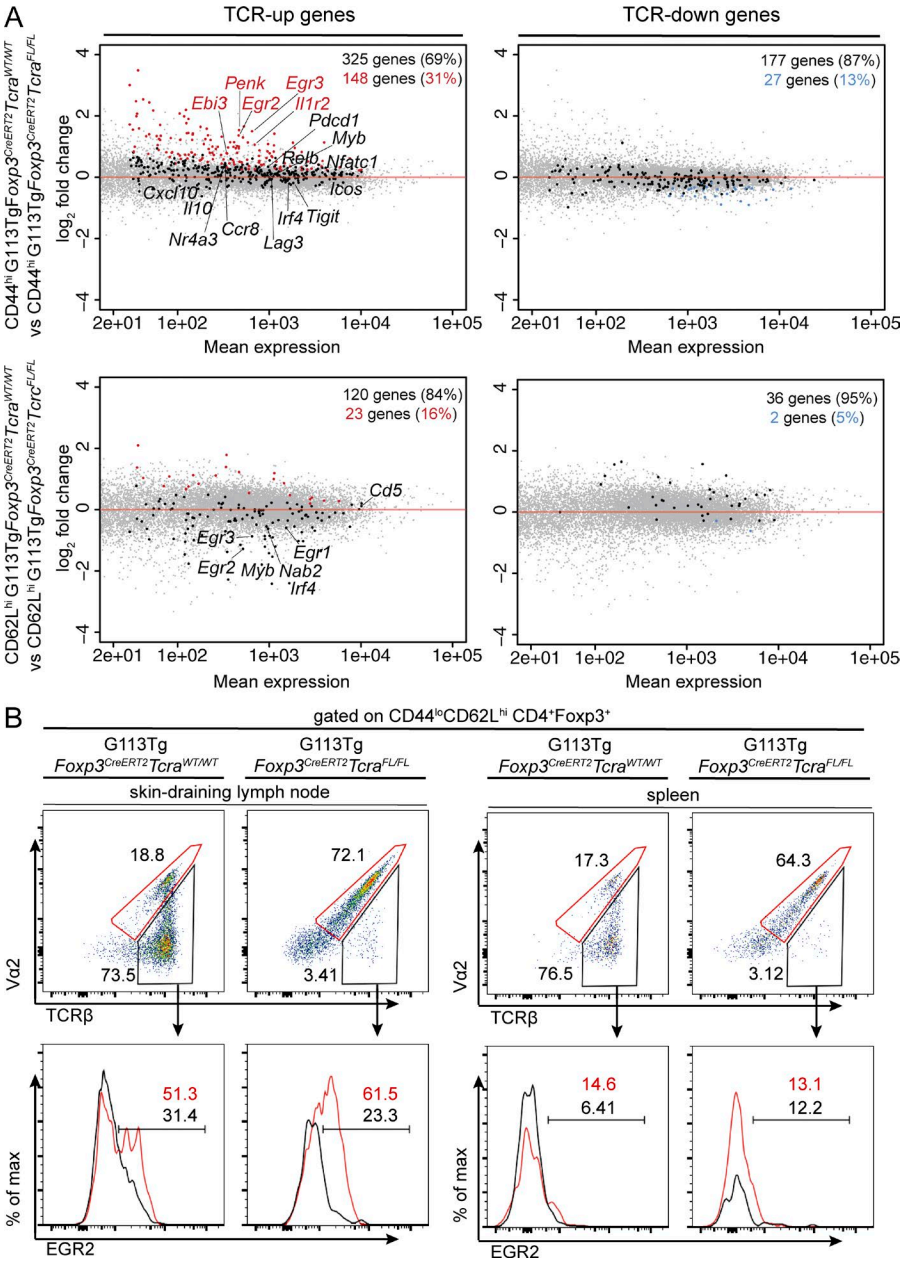

Figure 3. **Rescue of the polyclonal TCR-dependent gene signature in T reg cells upon expression of the monoclonal G113 TCR.** (A) *Foxp3*^{CreERT2}*Tcra*$^{FL/WT}$, *Foxp3*^{CreERT2}*Tcra*$^{FL/FL}$, G113Tg*Foxp3*^{CreERT2}*Tcra*$^{WT/WT}$, and G113Tg-*Foxp3*^{CreERT2}*Tcra*$^{FL/FL}$ mice were treated with tamoxifen on days 0, 1, and 7, and on day 9, the following populations were sorted from pooled spleens and lymph nodes of the indicated mice: CD44^{hi}CD62L^{lo} and CD44^{lo}CD62L^{hi} TCRβ^{+} and TCRβ^{-} eGFP^{+} T reg cells from *Foxp3*^{CreERT2}*Tcra*$^{FL/WT}$ mice; CD44^{hi}CD62L^{lo} and CD44^{lo}CD62L^{hi} TCRβ^{-} eGFP^{+} T reg cells from *Foxp3*^{CreERT2}*Tcra*$^{FL/FL}$ mice; CD44^{hi}CD62L^{lo} and CD44^{lo}CD62L^{hi} Vβ6^{+} eGFP^{+} T reg cells from G113Tg*Foxp3*^{CreERT2}*Tcra*$^{WT/WT}$ mice; and CD44^{hi}CD62L^{lo} and CD44^{lo}CD62L^{hi} Vβ6^{+}Vα2^{+} eGFP^{+} T reg cells from G113Tg*Foxp3*^{CreERT2}*Tcra*$^{FL/FL}$ mice. Strictly TCR-dependent genes were determined as described in the Rescue of the T reg cell TCR-dependent gene signature by monoclonal G113 TCR expression section of Results and discussion and were analyzed for significantly differential expression in the corresponding T reg cell subsets in G113Tg*Foxp3*^{CreERT2}*Tcra*$^{WT/WT}$ compared with G113Tg*Foxp3*^{CreERT2}*Tcra*$^{FL/FL}$ mice. Significantly TCR up-regulated genes (red; left) and TCR down-regulated genes (blue; right) are shown for effector (top) and naive (bottom) T reg cell subsets. Genes not significantly up-regulated (left) or down-regulated (right) are shown in black. All genes are shown in gray. Three replicates of each cell subset were generated, with at least five mice pooled for each replicate. A cutoff of 0.05 was set for the obtained p-values, adjusted using Benjamini-Hochberg multiple testing correction, to identify significant gene expression changes for each comparison. (B) Representative flow cytometric analyses of EGR2 expression in naive Vβ6^{+}Vα2^{-} (gates and histograms shown in black) and Vβ6^{+}Vα2^{+} (gates and histograms shown in red) T reg cells in pooled cervical, axial, brachial, and inguinal (skin draining) lymph nodes (left) and spleens (right) of tamoxifen-treated G113Tg-*Foxp3*^{CreERT2}*Tcra*$^{WT/WT}$ and G113Tg*Foxp3*^{CreERT2}*Tcra*$^{FL/FL}$ mice. Flow cytometry plots are representative of four independent experiments with at least three mice of each genotype per experiment.

Tcra$^{WT/WT}$ mice (Fig. 3 B). Even Vβ6^{+}Vα2^{+} G113^{+} T reg cells in G113Tg*Foxp3*^{CreERT2}*Tcra*$^{WT/WT}$ mice expressed more EGR2 than non-G113 Vβ6^{+}Vα2^{-} T reg cells in the same mice (Fig. 3 B). Notably, this was not the case in the splenic T reg cell subset (Fig. 3 B) nor was this true for T reg cells found in intestine-draining mesenteric or lung-draining mediastinal lymph nodes (not depicted). Thus, G113 TCR activation was evident only in the skin-draining cervical, axial, brachial, and inguinal lymph nodes. The same pattern was also observed for naive CD4 non–T reg cells expressing the G113 TCR (not depicted). TCR-dependent IRF4 expression assessed at a single-cell level showed a pattern similar to that of ERG2 (not depicted). These data suggested that the G113 TCR recognized endogenous antigen with an affinity significantly higher than the mean affinity of the polyclonal naive T reg and CD4 non–T reg cell TCR. Intriguingly, these data also suggested that endogenous antigen presentation in skin-draining lymph nodes allowed for greater activation of naive versus effec-

tor G113$^+$ T reg cells; we speculate this may be because of a limiting amount of antigen, perhaps presented by particular cells distributed throughout these secondary lymphoid organs such that their interactions with naive and effector cells are distinct. Finally, these data indicated that the G113 TCR likely recognized antigen predominantly expressed in the skin and consequently presented to naive G113$^+$ cells trafficking through skin-draining lymph nodes.

To further investigate this last possibility, we generated female G113Tg*Foxp3*$^{CreERT2/YFP\text{-}Cre}$*Tcra*$^{FL/FL}$ mice in which, because of X inactivation, half of the T reg cells express enhanced GFP (eGFP)–CreERT2 and half express YFP-Cre (YFP$^+$ cells; Fig. 4 A). We reasoned that in this setting, in the absence of tamoxifen treatment, where monoclonal Vβ6$^+$Vα2$^+$ G113$^+$ YFP$^+$ T reg cells compete with more diverse Vβ6$^+$Vα2$^-$ and Vβ6$^+$Vα2$^+$ eGFP-CreERT2$^+$ T reg cells, the lymph nodes and tissues expressing the highest amounts of the antigen recognized by the G113 TCR would enable accumulation and contain a relatively higher proportion of YFP$^+$ G113$^+$ T reg cells. Consistent with the idea of the G113 TCR recognizing primarily a skin-derived antigen, we observed preferential accumulation of YFP$^+$ Vβ6$^+$Vα2$^+$ T reg cells in skin-draining compared with intestine-draining mesenteric or lung-draining mediastinal lymph nodes (Fig. 4 A). YFP$^+$ cells as a percentage of total Foxp3$^+$ cells were also enriched in the skin itself, compared with in the intestine or lung (Fig. 4 B). To further confirm these results, we transferred fully polyclonal T reg cells isolated from *Foxp3*$^{Thy1.1}$ reporter mice and Vβ6$^+$Vα2$^+$ eGFP$^+$ T reg cells isolated from tamoxifen-treated G113Tg*Foxp3*^{CreERT2}*Tcra*$^{FL/FL}$ mice at a 1:1 ratio, together with congenically marked effector CD4 T cells, into T cell–deficient hosts. Assessment of the capacity of transferred T reg cells to accumulate in nonlymphoid tissues 2 wk later showed that Vβ6$^+$Vα2$^+$ G113-expressing T reg cells comprised a greater fraction of the T reg cell population in the skin compared with the intestine or the lung (Fig. 4 C).

To assess how expression of the G113 TCR might influence the localization of T reg cells within lymph nodes, we performed immunofluorescence analysis of secondary lymphoid organs in irradiated *Tcrb*$^{-/-}$/*Tcrd*$^{-/-}$ mice reconstituted with a 1:1 mix of T cell–depleted bone marrow cells from CD45.1$^+$ C57BL/6 and CD45.2$^+$ G113Tg*Foxp3*$^{YFP\text{-}Cre}$*Tcra*$^{FL/FL}$ mice to definitively identify monoclonal G113$^+$ T reg cells in situ in the absence of inflammation. In this setting, the majority of CD45.2$^+$CD4$^+$Foxp3$^-$ (as well as Foxp3$^+$) cells expressed both the transgenic Vβ6 and Vα2 chains and exhibited high EGR2 staining in skin-draining lymph nodes, consistent with productive signaling through the G113 TCR (Fig. 4 D). Consistent with flow cytometry data from G113Tg*Foxp3*$^{CreERT2/YFP\text{-}Cre}$*Tcra*$^{FL/FL}$ mice (Fig. 4 A), we observed an increased percentage of CD45.2$^+$ G113$^+$ T reg cells among total T reg cells in skin-draining compared with mesenteric or mediastinal lymph nodes (Fig. 4 E). Strikingly, clusters of CD45.2$^+$ cells significantly enriched in CD4$^+$Foxp3$^-$ and CD4$^+$Foxp3$^+$ T cells were apparent in skin-draining but not in mesenteric or mediastinal lymph nodes (Fig. 4, E–G). This result suggested antigen-dependent clustering of CD4$^+$ effector and T reg cells mutually expressing the G113 TCR.

Compared with CD45.1$^+$ polyclonal CD4$^+$ effector and T reg cells, CD45.2$^+$ CD4$^+$ effector and T reg cells, respectively, localized farther away from the center of the T cell zone in mesenteric and mediastinal but not in skin-draining lymph nodes, potentially indicating decreased antigen-dependent retention in the T cell zone (and increased exit through the medullary sinus) of G113$^+$ cells in non–skin-draining lymph nodes (Fig. 4, H and I). Thus, it is possible that antigen-dependent retention of G113$^+$ T reg cells (as opposed to increased proliferation) might account for their relative accumulation in skin-draining lymph nodes, as we did not observe increased percentages of Ki-67$^+$ Vβ6$^+$Vα2$^+$ YFP$^+$ T reg cells in skin-draining versus mesenteric or mediastinal lymph nodes in female G113Tg*Foxp3*$^{CreERT2/YFP\text{-}Cre}$*Tcra*$^{FL/FL}$ mice (not depicted).

Together, these data suggest that a single T reg cell TCR, with a specificity for a yet to be identified antigen, seemingly expressed predominantly in the skin, is sufficient to elicit the majority of the polyclonal TCR-dependent gene expression signature and support a life-sparing, even if partial, immunosuppressive function in T reg cells.

T reg cell function in the absence of developmentally selected TCR specificities

These observations raised the question whether provision of T reg cells with an irrelevant TCR specificity or specificities—rather than with a T reg cell–derived specificity—is also capable of providing some degree of immunosuppressive function. To address this question, we generated *Foxp3*$^{eGFP\text{-}CreERT2}$ mice, which harbor one *Tcra*^{FL} allele and one engineered conditional Vα14-Jα18 *Tcra* allele (Vahl et al., 2013). The latter enables expression of the Vα14-Jα18 NKT cell invariant TCRα chain in a Cre-inducible manner from an otherwise nonfunctional endogenous *Tcra* locus. Tamoxifen-induced activation of CreERT2 in *Foxp3*^{CreERT2}*Tcra*$^{FL/Vα14i\text{-}StopF}$ mice resulted in loss of endogenous TCRα expression from the *Tcra*^{FL} locus and induction of Vα14i chain expression from the *Tcra*$^{Vα14i\text{-}StopF}$ locus exclusively in T reg cells, effectively altering TCR specificity only in the T reg cells and leaving all other T cell populations fully polyclonal, i.e., equipped with their endogenous TCR repertoires (Fig. 5 A). Although all flipped Vα14i$^+$ T reg cells express the same TCRα chain, unperturbed endogenous TCRβ chain expression preserves considerable, albeit limited, diversity in these cells. Consistent with a lack of signaling downstream of Va14i$^+$ TCRs, the majority of Va14i$^+$ T reg cells in *Foxp3*^{CreERT2}*Tcra*$^{FL/Vα14i\text{-}StopF}$ mice did not express TCR-dependent factors such as EGR2 and IRF4; interestingly, however, a small percent did express these proteins indicative of productive TCR engagement (Fig. 5 A and not depicted). In vivo antibody-mediated CD1d blockade did not diminish expression levels of TCR-dependent genes in

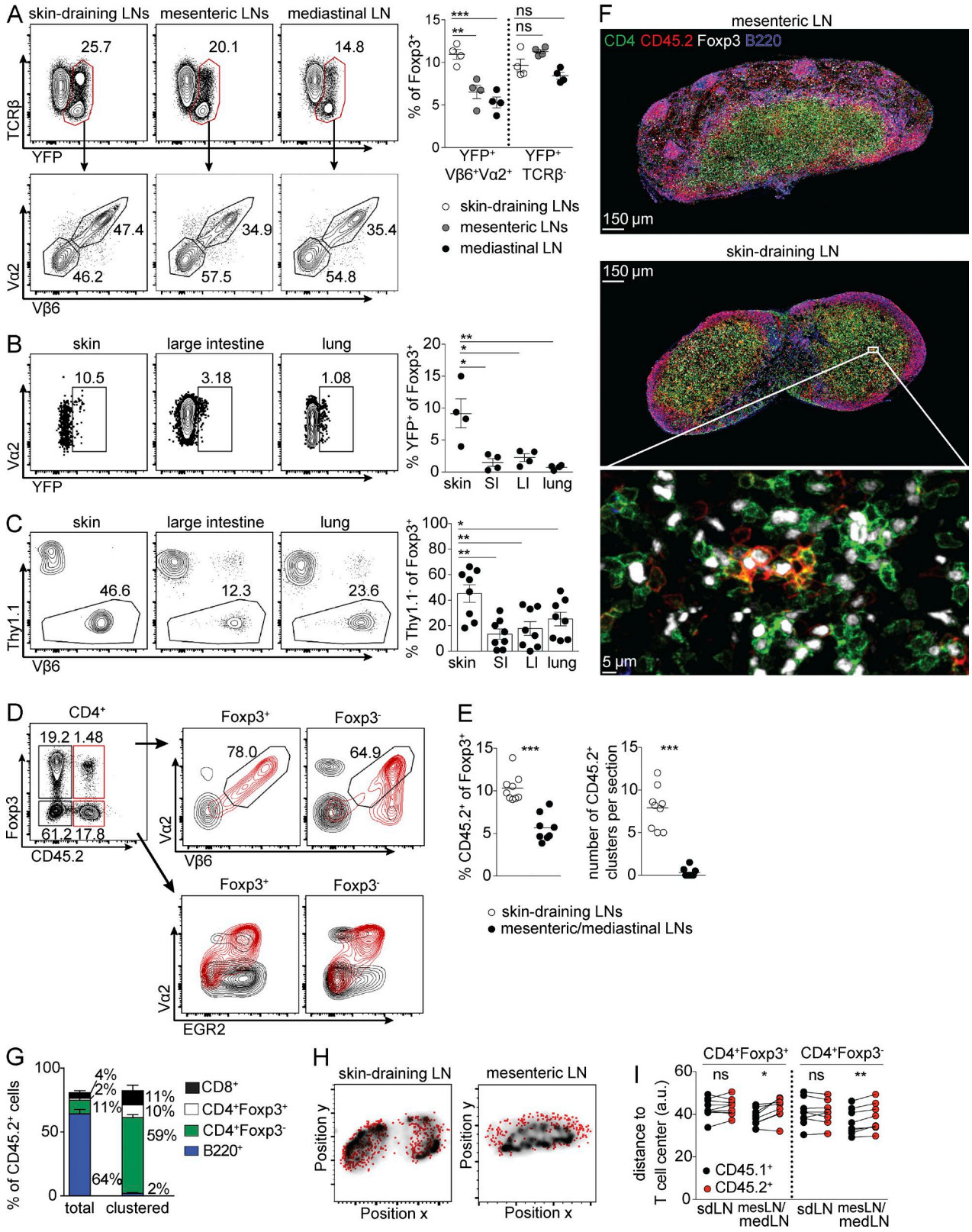

Figure 4. **Preferential accumulation of G113 TCR-expressing T reg cells in skin and draining lymph nodes.** (A) Flow cytometric analyses of CD4+ Foxp3+ cells (top left) in the indicated lymph nodes of female G113Tg*Foxp3*$^{CreERT2/YFP\text{-}Cre}$*Tcra*$^{FL/FL}$ mice. Further gating on YFP+ cells is shown below. (Right) The percent YFP+ Vβ6+Vα2+ and YFP+ TCRβ− cells among total Foxp3+ cells is quantified. (B, left) Representative flow cytometric analyses of CD4+Foxp3+

these cells, suggesting that such Vα14i$^+$ TCR signaling was likely caused by recognition of random ligands unrelated to T reg cell differentiation but not CD1d ligands recognized by NKT cell TCRs (not depicted). Analysis of the immune status in *Foxp3*^{CreERT2}*Tcra*$^{FL/Vα14i\text{-}StopF}$ mice 2 wk after tamoxifen administration revealed that T cell activation in *Foxp3*^{CreERT2} *Tcra*$^{FL/Vα14i\text{-}StopF}$ mice was to a large degree indistinguishable from that in *Foxp3*^{CreERT2}*Tcra*$^{FL/FL}$ mice, in which the majority of T reg cells do not express a TCR at all, with comparable percentages of CD44^{hi} and IFN-γ–, IL-2–, and IL-17–producing T cells (Fig. 5, C and D). Notably, however, lymphadenopathy was absent and Th2 cytokine production was markedly diminished in *Foxp3*^{CreERT2}*Tcra*$^{FL/Vα14i\text{-}StopF}$ relative to *Foxp3*^{CreERT2}*Tcra*$^{FL/FL}$ mice (Fig. 5, B and D). These data further suggest that certain aspects of immune activation can be controlled by T reg cells in a manner independent of their interactions with developmentally established cognate ligands and point to a more relaxed requirement for T reg cell TCR specificity for suppression of Th2 in comparison with Th1 responses.

Concluding remarks

Our study explored the requirement for a diverse TCR repertoire displayed by T reg cells for their suppressor function in vivo. Although a diverse repertoire in mature T reg cells was required for their ability to control Th1 immune responses and fully restrain tissue inflammation, a single TCR, expressed by T reg cells, did endow them with the capacity to suppress lymphadenopathy and, to a significant degree, Th2 and Th17 responses. It should be noted that, when transferred into T cell–deficient hosts, monoclonal T reg cells were also able to suppress Th1 responses in the lymph nodes; however, this was likely because of restraint of homeostatic proliferation of transferred T cells in the lymph nodes, which in this setting is required for Th1 responses.

T reg cells expressing the G113 TCR were able to markedly extend the lifespan of mice by restraining fatal early onset autoimmune disease resulting from congenital or induced T reg cell deficiency or from ablation of TCR expression in T reg cells (Fontenot et al., 2003; Kim et al., 2007; Levine et al., 2014). However, at the same time, rescue of tolerance was far from complete, as even in young G113Tg*Foxp3*$^{YFP\text{-}Cre}$*Tcra*$^{FL/FL}$ mice, marked tissue pathology was apparent. Consistent with functional studies, expression of this single monoclonal T reg cell–derived TCR was able to support the majority, but not all, of gene expression features imparted by a diverse T reg TCR repertoire. These findings suggested that a diverse T reg cell TCR mosaic was required for activation of T reg cells in specific geographical locations, rather than for enabling expression of distinct gene subsets induced in an individual TCR specificity–dependent manner and involved either directly or indirectly in elaboration of suppressor function. This notion was supported by the observed preferential stimulation and clustering of T reg cells expressing the monoclonal G113 TCR in skin-draining lymph nodes, where they also seemed to preferentially exert their suppressor function. An additional and nonmutually exclusive possibility was that suppression of immune responses in the lymph nodes and of Th2 cell activation has less stringent requirements for diverse TCR-dependent interactions between T reg cells and their developmentally established cognate antigens, as opposed to Th1 responses whose suppression by T reg cells may more strictly require diverse, specific, and, perhaps, increased affinity T reg cell TCR–ligand interactions. The latter possibility is supported by our observation that *Foxp3*^{CreERT2} *Tcra*$^{FL/Vα14i\text{-}StopF}$ mice with TCRs not selected in the thymus lack lymphadenopathy and exhibit selectively diminished Th2 responses compared with *Foxp3*^{CreERT2}*Tcra*$^{FL/FL}$ littermates.

Limited autoimmunity caused by incomplete CreERT2-mediated deletion and potentially confounding effects of G113Tg expression precluded a more nuanced assessment of whether Va14i$^+$ T reg cells in *Foxp3*^{CreERT2} *Tcra*$^{FL/Vα14i\text{-}StopF}$ mice were less suppressive than G113$^+$ T reg cells in G113Tg*Foxp3*^{CreERT2}*Tcra*$^{FL/FL}$ mice. Furthermore, consistent with minimal antigen-dependent TCR stimulation of flipped Va14i$^+$ T reg cells in vivo, we found that in

cells isolated from tissues of G113Tg*Foxp3*$^{CreERT2/YFP\text{-}Cre}$*Tcra*$^{FL/FL}$ mice. (Right) Quantification of YFP$^+$ cells within the total Foxp3$^+$ cell population. (C) 4×10^5 Thy1.1$^+$ cells from *Foxp3*$^{Thy1.1}$ mice, 4×10^5 Vβ6$^+$Vα2$^+$ eGFP$^+$ cells from tamoxifen-treated G113Tg*Foxp3*^{CreERT2}*Tcra*$^{FL/FL}$ mice, and 1.6×10^6 CD45.1$^+$eGFP$^-$ cells from CD45.1$^+$Foxp3^{GFP} mice were transferred into *Tcrb*$^{-/-}$/*Tcrd*$^{-/-}$ mice analyzed 2 wk later. (Left) Representative flow cytometric analysis of Thy1.1$^+$ and Thy1.1$^-$ (Vβ6$^+$Vα2$^+$) T reg cells in the indicated tissues. (Right) The proportion of Thy1.1$^-$ cells (percentage) among total Foxp3$^+$ cells. (D) Representative flow cytometric analyses from an inguinal lymph node of bone marrow chimeric mice. (Right) Plots of the indicated populations of CD45.2$^+$ (red) and CD45.2$^-$ (black) Foxp3$^+$ (left) and Foxp3$^-$ (right) cells, with gates indicating the percent Vβ6$^+$Vα2$^+$ cells among CD45.2$^+$ Foxp3$^+$ and Foxp3$^-$ populations. (E) Percent CD45.2$^+$ among Foxp3$^+$ cells (left) and numbers of CD45.2$^+$ clusters per imaged section (right) in skin-draining (open circles) or mesenteric/mediastinal (closed circles) lymph nodes. (F) Representative immunofluorescence staining of lymph nodes as indicated. (G) Percent CD8$^+$ (black bars), CD4$^+$Foxp3$^-$ (green bars), CD4$^+$Foxp3$^+$ (white bars), and B220$^+$ (blue bars) cells of CD45.2$^+$ cells in skin-draining lymph nodes (total) or in CD45.2$^+$ clusters (clustered) in skin-draining lymph nodes. Error bars represent ± SEM. (H) Representative images showing localization of CD45.1$^+$ (black contours) and CD45.2$^+$ (red dots) Foxp3$^+$ cells in the indicated lymph nodes. (I) Quantification of data in H for both CD4$^+$Foxp3$^+$ and CD4$^+$Foxp3$^-$ cells. (A–C) Each circle represents an individual mouse. (A and B) The data are representative of at least two independent experiments with at least two mice of each genotype per experimental group. (C) The data represents the combined results of two experiments with four mice per group each. (D–I) The data are the combined results from the analysis of two independent experiments with a total of three individual mice. (E and I) Each circle represents an imaged section. P-values were calculated using unpaired (A–E) or paired (I) Student's *t* test. *, $P < 0.05$; **, $P < 0.01$; ***, $P < 0.001$. a.u., arbitrary units; LI, large intestine; medLN, mediastinal lymph node; mesLN, mesenteric lymph node; sdLN, skin-draining lymph node; SI, small intestine.

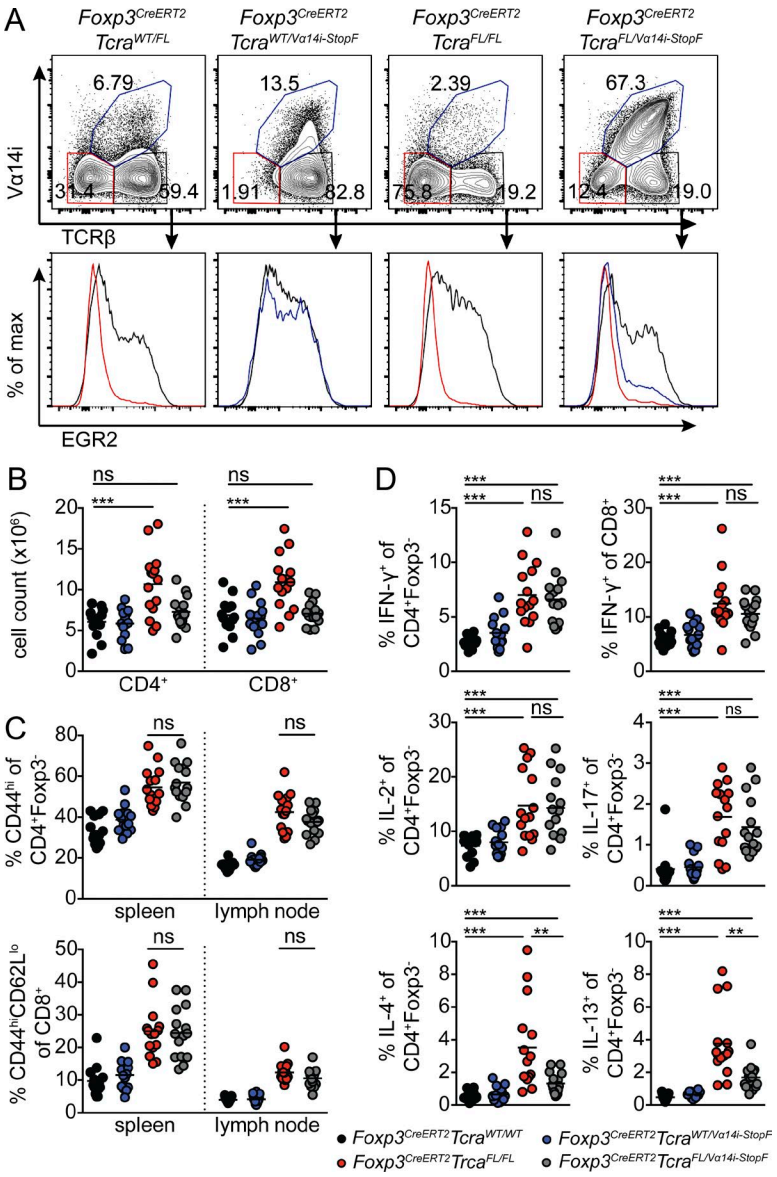

Figure 5. **Limited T reg cell function in the absence of developmentally established TCR specificities.** (A, top) Representative flow cytometric analyses of lymph nodes from mice of the indicated genotypes, gated on CD4$^+$Foxp3$^+$ cells. (Bottom) EGR2 staining is shown for the indicated cell populations (red, TCRβ$^-$; black, TCRβ$^+$; blue, Vα14i$^+$). (B–D) Lymph node cellularity (B), T cell activation status (C), and splenic T cell cytokine production (D) in *Foxp3*^{CreERT2}*Tcra*$^{WT/WT}$ (black circles), *Foxp3*^{CreERT2}*Tcra*$^{WT/Vα14i\text{-}StopF}$ (blue circles), *Foxp3*^{CreERT2}*Tcra*$^{FL/FL}$ (red circles), and *Foxp3*^{CreERT2}*Tcra*$^{FL/Vα14i\text{-}StopF}$ (gray circles) mice. Each circle represents an individual mouse. P-values were calculated using unpaired Student's *t* test. **, P < 0.01; ***, P < 0.001. (A) The data are representative of two independent experiments with at least two mice per genotype each. (B–D) Data represent the combined results of three experiments with at least four mice per group each.

Foxp3$^{YFP\text{-}Cre}$*Tcra*$^{FL/Vα14i\text{-}StopF}$ mice, the residual non-flipped Va14i$^-$ T reg cells outcompeted flipped Va14i$^+$ cells in the periphery and were present in substantial numbers. These expanded cells expressing an endogenous TCR repertoire prevented autoimmunity and impeded a direct comparison of T reg cell function in *Foxp3*$^{YFP\text{-}Cre}$*Tcra*$^{FL/Vα14i\text{-}StopF}$ and G113Tg*Foxp3*$^{YFP\text{-}Cre}$*Tcra*$^{FL/FL}$ mice (not depicted). Nevertheless, our analyses of two different genetic means of perturbation of the T reg cell TCR repertoire suggest distinct requirements for T reg cell TCR specificity for suppression of Th1 versus Th2 responses. These findings parallel previous observations that Th1 effector cell differentiation is facilitated by TCR engagement of higher affinity or avidity in comparison with those supporting generation of Th2 cells (Constant et al., 1995; van Panhuys et al., 2014).

MATERIALS AND METHODS

Mice

Foxp3$^{YFP\text{-}Cre}$ (Rubtsov et al., 2008), *Foxp3*$^{eGFP\text{-}CreERT2}$ (Rubtsov et al., 2010), *Tcra*^{FL} (Polic et al., 2001), *Foxp3*^{KO} (Fontenot et al., 2003), G113Tg (Bautista et al., 2009), *Foxp3*^{DTReGFP} (Kim et al., 2007), and *Tcra*$^{FL/Vα14i\text{-}StopF}$ (Vahl et al., 2013) mice have been previously described. CD45.1 and *Tcrb*$^{-/-}$*Tcrd*$^{-/-}$ mice were purchased from The Jackson Laboratory. Mice were sex and age matched in all experiments, with the exception of experiments involving only female G113Tg*Foxp3*$^{CreERT2/YFP\text{-}Cre}$*Tcra*$^{FL/FL}$ mice. Generation and treatments of mice were performed under protocol 08–10-023 approved by the Sloan Kettering Institute Institutional Animal Care and Use Committee. All mouse strains were maintained in the Sloan Kettering Institute animal facility

in specific pathogen–free conditions in accordance with institutional guidelines.

For tamoxifen administration, 40 mg tamoxifen dissolved in 100 µl ethanol and subsequently in 900 µl olive oil (Sigma-Aldrich) was sonicated 4 × 30 s in a Bioruptor Twin system (Diagenode). Mice were orally gavaged with 200 µl tamoxifen emulsion per treatment. For diphtheria toxin (DT) injections, DT (Sigma-Aldrich) was dissolved in PBS, and 200 µl (5 µg/ml) were injected i.p. per mouse.

Isolation of cells

Spleens and lymph nodes were dissociated using ground glass slides and filtered. Red blood cells in spleens were lysed before analysis. To isolate lymphocytes from tissues, mice were euthanized and immediately perfused with 20 ml PBS. Small and large intestines were removed and flushed with PBS, Peyer's patches were removed, and residual fat and connective tissue were removed. Intestines were opened lengthwise and cut into 0.5-cm–long pieces that were further washed by vortexing in PBS. Samples were incubated in PBS supplemented with 5% fetal calf serum, 1% L-glutamine, 1% penicillin-streptomycin, 10 mM Hepes, 1 mM dithiothreitol, and 1 mM EDTA for 15 min to dissociate intraepithelial lymphocytes, which were discarded. Samples were washed and incubated in digest solution (RPMI medium supplemented with 5% fetal calf serum, 1% L-glutamine, 1% penicillin-streptomycin, 10 mM Hepes, 1 mg/ml collagenase, and 1 U/ml DNase I) for 10 min. Cells were collected through a 100-µm strainer, and the residual samples were incubated in digest solution again for 10 min before filtering through 100-µm strainers and combining with previously collected cells. Cells were resuspended in 35% Percoll to eliminate debris before resuspension in staining buffer. To isolate lymphocytes from skin and lungs, tissues were physically dissociated using scissors and incubated for 50–60 min in digest solution before being filtered through 100-µm strainers. Samples were resuspended in 35% Percoll to eliminate debris before resuspension in staining buffer.

Cell transfer experiments

For cell transfer experiments, pooled spleens and lymph nodes were enriched for CD4 T cells using the Dynabeads CD4 Positive Isolation kit. Cells were FACS sorted on an Aria II cell sorter (BD), washed three times in PBS, resuspended in 200 µl PBS, and transferred into recipients via retroorbital injection.

Flow cytometric analysis

Cells were stained with LIVE/DEAD Fixable Yellow Dead Cell stain (Molecular Probes) and the following antibodies purchased from eBioscience, BioLegend, BD, or Tonbo or obtained from the National Institutes of Health tetramer core facility: anti-CD4 (RM4-5), anti-CD8a (5H10), anti-TCRβ (H57-597), anti-Vβ6 (RR4-7), anti-Vα2 (B20.1), EGR2 (erongr2), IRF4 (E3 4), IL-1R2 (4E2), PBS-57–loaded mCD1d tetramer, anti-CD44 (IM7), anti-CD62L (MEL-14), anti-CD25 (PC61), anti-Foxp3 (FJK-16s), anti–IFN-γ (XMG1.2), anti–IL-4 (11B11), anti–IL-13 (eBio13A), anti–IL-17A (17B7), and anti–IL-2 (JES6-5H4). A monoclonal anti-Vα14i antibody (NKT14) was provided by F. Scheuplein and R. Schaub (NKT Therapeutics, Waltham, MA; Scheuplein et al., 2015). Flow cytometric analysis was performed using an LSRII flow cytometer (BD) and FlowJo software (Tree Star). Intracellular staining was performed using eBioscience Fixation Permeabilization buffers. For cytokine staining, lymphocytes were stimulated with 5 µg/ml soluble anti-CD3 clone 2C11 and 5 µg/ml anti-CD28 clone 37.51 in the presence of 1 µg/ml brefeldin A for 5 h at 37°C and 5% CO_2.

RNA-seq analysis

Foxp3^{CreERT2}*Tcra*$^{FL/WT}$, *Foxp3*^{CreERT2}*Tcra*$^{FL/FL}$, G113Tg*Foxp3*^{CreERT2}*Tcra*$^{WT/WT}$, and G113Tg*Foxp3*^{CreERT2}*Tcra*$^{FL/FL}$ mice were treated with tamoxifen on days 0, 1, 7, and 9, and after CD4 T cell enrichment from pooled lymph nodes and spleens using the Dynabeads CD4 Positive Isolation kit, the following populations were sorted from the indicated mice and resuspended in TRIzol: CD44^{hi}CD62L^{lo} and CD44^{lo}CD62L^{hi} TCRβ^{+} and TCRβ^{-} T reg cells from *Foxp3*^{CreERT2}*Tcra*$^{FL/WT}$ mice, CD44^{hi}CD62L^{lo} and CD44^{lo}CD62L^{hi} TCRβ^{+} and TCRβ^{-} T reg cells from *Foxp3*^{CreERT2}*Tcra*$^{FL/FL}$ mice, CD44^{hi}CD62L^{lo} and CD44^{lo}CD62L^{hi} Vβ6^{+} T reg cells from G113Tg*Foxp3*^{CreERT2}*Tcra*$^{WT/WT}$ mice, and CD44^{hi}CD62L^{lo} and CD44^{lo}CD62L^{hi} Vβ6^{+}Vα2^{+} T reg cells from G113Tg-*Foxp3*^{CreERT2}*Tcra*$^{FL/FL}$ mice. Three replicates of each cell subset (at least five mice per replicate) were generated. RNA-seq reads were aligned to the reference mouse genome GRCm38 using the Burrows-Wheeler Aligner (Li and Durbin, 2010), and local realignment was performed using the Genome Analysis Toolkit (McKenna et al., 2010). For each sample, raw count of reads per gene was measured using R, and DESeq2 R package (Love et al., 2014) was used to perform differential gene expression among different conditions. A cutoff of 0.05 was set on the obtained p-values (that were adjusted using Benjamini-Hochberg multiple testing correction) to get the significant genes of each comparison.

Immunofluorescence and histocytometry

Immunofluorescence and histocytometry were performed as previously described (Liu et al., 2015). In brief, lymph nodes were harvested, fixed in 1% paraformaldehyde containing buffer, and dehydrated in 30% sucrose before embedding in optimal cutting temperature freezing media (Sakura). 20-µm sections were subsequently prepared and stained overnight at 4°C with combinations of the following antibodies purchased from eBioscience, BioLegend, or BD: B220 (RA3-6B2), CD3 (17A2), CD4 (GK1.5 or RM4-5), CD8 (53-6.7), CD45.1 (A20), CD45.2 (104), and Foxp3 (FJK-16s).

Multicolor confocal images were acquired on a confocal microscope (SP8; Leica Biosystems) equipped with a 40×/1.3 NA oil objective (Leica Biosystems). The result-

ing images were subsequently corrected for fluorophore spillover using the Leica channel dye separation module (Application Suite X software; Leica Biosystems), deconvolved in Huygen's Essential software (Scientific Volume Imaging), and further processed in Imaris software (Bitplane). Identification of CD45.2$^+$ clusters was conducted using the CD45.2 channel for surface creation without object splitting (Imaris surface creation wizard module). Surfaces with a volume above a threshold curated visually were subsequently used to create a novel binary clustered versus nonclustered channel. Nest, nuclear-based cellular segmentation was performed either on total nuclei stained with the DNA dye Jojo1 (Thermo Fisher Scientific) or on Foxp3$^+$ nuclei. Object statistics were exported into FlowJo X (Tree Star) for analysis.

Minimum distance measurements between points of interest were computed as previously described (Gerner et al., 2012) using the formula: d = sqrt [(x1 − x2)^2 + (y1 − y2)^2] and finding its minimum in Excel (Microsoft). For each lymph node, the T cell area centroid coordinates were used as reference points for these calculations. For normalization across multiple lymph nodes of different volumes and shapes, the distance between the remotest T reg and the T cell zone center for each lymph node was introduced as the normalization factor for the subsequent statistical analysis.

Statistical analysis

All statistical analyses (excluding RNA-seq analyses, described in the Rescue of the T reg cell TCR-dependent gene signature by monoclonal G113 TCR expression section) were performed using Prism 6 (GraphPad Software). Differences between individual groups were analyzed for statistical significance using unpaired or paired two-tailed Student's *t* tests. *, $P \geq 0.05$; **, $P \geq 0.01$; ***, $P \geq 0.001$.

ACKNOWLEDGMENTS

We thank members of the Rudensky laboratory for critical discussions and A.H. Bravo and S.E. Lee for experimental support. We thank Felix Scheuplein and Robert Schaub for generously providing the anti-Vα14i antibody (NKT14).

This work was supported by a National Institutes of Health (NIH) Medical Scientist Training Program grant (T32GM07739) to the Weill Cornell/Rockefeller/Sloan-Kettering Tri-Institutional MD-PhD Program (A.G. Levine), the Frank Lappin Horsfall Jr. Student Fellowship (A.G. Levine), an NIH grant (R37AI034206 to A.Y. Rudensky), the Ludwig Center at Memorial Sloan-Kettering Cancer Center, the Hilton-Ludwig Cancer Prevention Initiative of the Conrad N. Hilton Foundation and Ludwig Cancer Research (A.Y. Rudensky), and the NIH/National Cancer Institute Cancer Center Support Grant (P30 CA008748). This research was also supported in part by the Intramural Research Program of the National Institute of Allergy and Infectious Diseases, NIH (R.N. Germain and A.P. Baptista). A.Y. Rudensky is an investigator with the Howard Hughes Medical Institute.

The authors declare no competing financial interests.

Author contributions: A.G. Levine and A.Y. Rudensky conceived the study, designed experiments, and wrote the manuscript, with final edits involving A.P. Baptista and R.N. Germain. A.G. Levine performed experiments and analyzed data. S. Hemmers assisted with some experiments. A.P. Baptista performed immunofluorescence analysis. R.N. Germain discussed experimental imaging plans and data interpretation. M. Schizas and C. Konopacki performed RNA-seq data analysis. M.B. Faire and B. Moltedo assisted with in vitro experiments. M. Schmidt-Supprian provided Tcra$^{Vα14i\text{-}StopF}$ mice. P.M. Treuting performed histological analyses.

Submitted: 12 August 2016
Revised: 6 November 2016
Accepted: 23 December 2016

REFERENCES

Anderson, M.S., E.S. Venanzi, L. Klein, Z. Chen, S.P. Berzins, S.J. Turley, H. von Boehmer, R. Bronson, A. Dierich, C. Benoist, and D. Mathis. 2002. Projection of an immunological self shadow within the thymus by the aire protein. *Science.* 298:1395–1401. http://dx.doi.org/10.1126/science.1075958

Bautista, J.L., C.W. Lio, S.K. Lathrop, K. Forbush, Y. Liang, J. Luo, A.Y. Rudensky, and C.S. Hsieh. 2009. Intraclonal competition limits the fate determination of regulatory T cells in the thymus. *Nat. Immunol.* 10:610–617. http://dx.doi.org/10.1038/ni.1739

Constant, S., C. Pfeiffer, A. Woodard, T. Pasqualini, and K. Bottomly. 1995. Extent of T cell receptor ligation can determine the functional differentiation of naive CD4+ T cells. *J. Exp. Med.* 182:1591–1596. http://dx.doi.org/10.1084/jem.182.5.1591

Feng, Y., J. van der Veeken, M. Shugay, E.V. Putintseva, H.U. Osmanbeyoglu, S. Dikiy, B.E. Hoyos, B. Moltedo, S. Hemmers, P. Treuting, et al. 2015. A mechanism for expansion of regulatory T-cell repertoire and its role in self-tolerance. *Nature.* 528:132–136. http://dx.doi.org/10.1038/nature16141

Fontenot, J.D., M.A. Gavin, and A.Y. Rudensky. 2003. Foxp3 programs the development and function of CD4$^+$CD25$^+$ regulatory T cells. *Nat. Immunol.* 4:330–336. http://dx.doi.org/10.1038/ni904

Gerner, M.Y., W. Kastenmuller, I. Ifrim, J. Kabat, and R.N. Germain. 2012. Histo-cytometry: a method for highly multiplex quantitative tissue imaging analysis applied to dendritic cell subset microanatomy in lymph nodes. *Immunity.* 37:364–376. http://dx.doi.org/10.1016/j.immuni.2012.07.011

Hsieh, C.S., Y. Liang, A.J. Tyznik, S.G. Self, D. Liggitt, and A.Y. Rudensky. 2004. Recognition of the peripheral self by naturally arising CD25$^+$ CD4$^+$ T cell receptors. *Immunity.* 21:267–277. http://dx.doi.org/10.1016/j.immuni.2004.07.009

Hsieh, C.S., Y. Zheng, Y. Liang, J.D. Fontenot, and A.Y. Rudensky. 2006. An intersection between the self-reactive regulatory and nonregulatory T cell receptor repertoires. *Nat. Immunol.* 7:401–410. http://dx.doi.org/10.1038/ni1318

Jordan, M.S., A. Boesteanu, A.J. Reed, A.L. Petrone, A.E. Holenbeck, M.A. Lerman, A. Naji, and A.J. Caton. 2001. Thymic selection of CD4$^+$CD25$^+$ regulatory T cells induced by an agonist self-peptide. *Nat. Immunol.* 2:301–306. http://dx.doi.org/10.1038/86302

Killebrew, J.R., N. Perdue, A. Kwan, A.M. Thornton, E.M. Shevach, and D.J. Campbell. 2011. A self-reactive TCR drives the development of Foxp3$^+$ regulatory T cells that prevent autoimmune disease. *J. Immunol.* 187:861–869. http://dx.doi.org/10.4049/jimmunol.1004009

Kim, J.M., J.P. Rasmussen, and A.Y. Rudensky. 2007. Regulatory T cells prevent catastrophic autoimmunity throughout the lifespan of mice. *Nat. Immunol.* 8:191–197. http://dx.doi.org/10.1038/ni1428

Leung, M.W., S. Shen, and J.J. Lafaille. 2009. TCR-dependent differentiation of thymic Foxp3$^+$ cells is limited to small clonal sizes. *J. Exp. Med.* 206:2121–2130. http://dx.doi.org/10.1084/jem.20091033

Leventhal, D.S., D.C. Gilmore, J.M. Berger, S. Nishi, V. Lee, S. Malchow, D.E. Kline, J. Kline, D.J. Vander Griend, H. Huang, et al. 2016. Dendritic cells coordinate the development and homeostasis of organ-specific regulatory T cells. *Immunity.* 44:847–859. http://dx.doi.org/10.1016/j.immuni.2016.01.025

Levine, A.G., A. Arvey, W. Jin, and A.Y. Rudensky. 2014. Continuous requirement for the TCR in regulatory T cell function. *Nat. Immunol.* 15:1070–1078. http://dx.doi.org/10.1038/ni.3004

Li, H., and R. Durbin. 2010. Fast and accurate long-read alignment with Burrows-Wheeler transform. *Bioinformatics.* 26:589–595. http://dx.doi.org/10.1093/bioinformatics/btp698

Lin, J., L. Yang, H.M. Silva, A. Trzeciak, Y. Choi, S.R. Schwab, M.L. Dustin, and J.J. Lafaille. 2016. Increased generation of Foxp3$^+$ regulatory T cells by manipulating antigen presentation in the thymus. *Nat. Commun.* 7:10562. http://dx.doi.org/10.1038/ncomms10562

Liu, Z., M.Y. Gerner, N. Van Panhuys, A.G. Levine, A.Y. Rudensky, and R.N. Germain. 2015. Immune homeostasis enforced by co-localized effector and regulatory T cells. *Nature.* 528:225–230. http://dx.doi.org/10.1038/nature16169

Love, M.I., W. Huber, and S. Anders. 2014. Moderated estimation of fold change and dispersion for RNA-seq data with DESeq2. *Genome Biol.* 15:550. http://dx.doi.org/10.1186/s13059-014-0550-8

Malchow, S., D.S. Leventhal, V. Lee, S. Nishi, N.D. Socci, and P.A. Savage. 2016. Aire enforces immune tolerance by directing autoreactive T cells into the regulatory T cell lineage. *Immunity.* 44:1102–1113. http://dx.doi.org/10.1016/j.immuni.2016.02.009

McKenna, A., M. Hanna, E. Banks, A. Sivachenko, K. Cibulskis, A. Kernytsky, K. Garimella, D. Altshuler, S. Gabriel, M. Daly, and M.A. DePristo. 2010. The Genome Analysis Toolkit: a MapReduce framework for analyzing next-generation DNA sequencing data. *Genome Res.* 20:1297–1303. http://dx.doi.org/10.1101/gr.107524.110

Moran, A.E., K.L. Holzapfel, Y. Xing, N.R. Cunningham, J.S. Maltzman, J. Punt, and K.A. Hogquist. 2011. T cell receptor signal strength in T_{reg} and iNKT cell development demonstrated by a novel fluorescent reporter mouse. *J. Exp. Med.* 208:1279–1289. http://dx.doi.org/10.1084/jem.20110308

Polic, B., D. Kunkel, A. Scheffold, and K. Rajewsky. 2001. How αβ T cells deal with induced TCR α ablation. *Proc. Natl. Acad. Sci. USA.* 98:8744–8749. http://dx.doi.org/10.1073/pnas.141218898

Rubtsov, Y.P., J.P. Rasmussen, E.Y. Chi, J. Fontenot, L. Castelli, X. Ye, P. Treuting, L. Siewe, A. Roers, W.R. Henderson Jr., et al. 2008. Regulatory T cell-derived interleukin-10 limits inflammation at environmental interfaces. *Immunity.* 28:546–558. http://dx.doi.org/10.1016/j.immuni.2008.02.017

Rubtsov, Y.P., R.E. Niec, S. Josefowicz, L. Li, J. Darce, D. Mathis, C. Benoist, and A.Y. Rudensky. 2010. Stability of the regulatory T cell lineage in vivo. *Science.* 329:1667–1671. http://dx.doi.org/10.1126/science.1191996

Samy, E.T., L.A. Parker, C.P. Sharp, and K.S. Tung. 2005. Continuous control of autoimmune disease by antigen-dependent polyclonal CD4$^+$CD25$^+$ regulatory T cells in the regional lymph node. *J. Exp. Med.* 202:771–781. http://dx.doi.org/10.1084/jem.20041033

Scheuplein, F., D.J. Lamont, M.E. Poynter, J.E. Boyson, D. Serreze, L.K. Lundblad, R. Mashal, and R. Schaub. 2015. Mouse invariant monoclonal antibody NKT14: A novel tool to manipulate iNKT cell function in vivo. *PLoS One.* 10:e0140729. http://dx.doi.org/10.1371/journal.pone.0140729

Vahl, J.C., K. Heger, N. Knies, M.Y. Hein, L. Boon, H. Yagita, B. Polic, and M. Schmidt-Supprian. 2013. NKT cell-TCR expression activates conventional T cells in vivo, but is largely dispensable for mature NKT cell biology. *PLoS Biol.* 11:e1001589. http://dx.doi.org/10.1371/journal.pbio.1001589

Vahl, J.C., C. Drees, K. Heger, S. Heink, J.C. Fischer, J. Nedjic, N. Ohkura, H. Morikawa, H. Poeck, S. Schallenberg, et al. 2014. Continuous T cell receptor signals maintain a functional regulatory T cell pool. *Immunity.* 41:722–736. http://dx.doi.org/10.1016/j.immuni.2014.10.012

van Panhuys, N., F. Klauschen, and R.N. Germain. 2014. T-cell-receptor-dependent signal intensity dominantly controls CD4$^+$ T cell polarization in vivo. *Immunity.* 41:63–74. http://dx.doi.org/10.1016/j.immuni.2014.06.003

Yang, S., N. Fujikado, D. Kolodin, C. Benoist, and D. Mathis. 2015. Regulatory T cells generated early in life play a distinct role in maintaining self-tolerance. *Science.* 348:589–594. http://dx.doi.org/10.1126/science.aaa7017